

A Study on the Convergence Behaviour of the Hybrid Coarse Mesh Finite Difference (HCMFD) Method

Tae-suk Oh ^a and Yonghee Kim ^{a*}

^aKorea Advanced Institute of Science and Technology, 291 Daehak-ro, Yuseong-gu, Daejeon 34141, Korea

*Corresponding author: yongheekim@kaist.ac.kr

1. Introduction

In order to harness the distribution of neutron flux within a reactor system of interest, either transport or diffusion equations can be utilized. A solution from the former method results in an accurate estimation but often requires strenuous computation, whereas the latter approach can be cheaply solved but presents an inherent limit in its accuracy.

For synergistic exploitation of aforementioned approaches, a concept of two-step procedure had been devised. The heterogeneity of each fuel assembly is dealt through high fidelity transport calculation and represented through assembly-wise homogenized quantities [1]. The whole core can then be expressed through such parameters, where assembly-wise diffusion calculation can be applied to acquire its attribute.

However, due to the assembly-wise homogenization, approximation is imperative to estimate the pin wise information for such a conventional two-step approach. Hence, an attention toward the pin-wise two-step procedure is being recognized, but such a procedure will entail a noticeable computational burden that stems from the enlargement of the system matrix to be handled.

Recently, a novel acceleration scheme for pin-wise nodal calculation had been proposed, namely Hybrid Coarse-Mesh Finite Difference (HCMFD) method [2,3]. The assembly-wise (global) nodes comprise the reactor eigenvalue problem, whereas the pin-wise (local) nodes formulate an assembly-wise fixed-source problem. Whereupon, a hierarchy of acceleration can be established, which maximizes the parallel efficiency.

In this work, a scrutiny concerning the convergence behaviour of such a method has been conducted, which reveals a strong dependency on how the local calculation is treated. Especially, for stainless steel reflected MOX fuel embedded core, an inflection in the convergence of source error was observed. The details along with the heuristic remedy to circumvent such an anomaly are discussed.

2. Hybrid Coarse-Mesh Finite Difference Method

The Hybrid CMFD method is devised for pin-wise nodal analysis which considers two different types of nodes: global and local nodes associated with assembly and pin-wise homogenized parameters respectively.

The one-node CMFD acceleration is applied on global nodes and the conventional CMFD acceleration is utilized for local nodes to establish a parallelized acceleration structure [2].

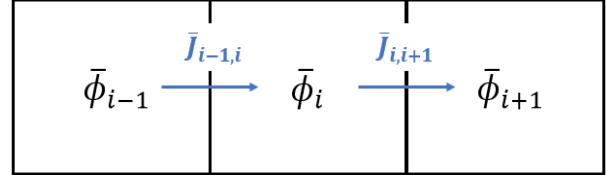


Fig. 1. Balance within a node of interest.

2.1 CMFD Method

Balance for neutron flux within a node of interest i as shown in Fig. 1 can be expressed as below:

$$\bar{J}_{i,i+1} - \bar{J}_{i-1,i} + \Sigma_{ri}\Delta x_i \bar{\phi}_i = \frac{\chi_{gi}}{k} \sum_g v \Sigma_{fg} \Delta x_i \bar{\phi}_i, \quad (1)$$

where $\bar{J}_{i,i+1}$ represents the net neutron current egressing from node i toward the adjacent node $i+1$, k denotes the multiplication factor, and all the other notations are that of the convention. Through finite difference method (FDM), one yields the following simple relations:

$$\bar{J}_{i,i+1} = -\bar{D}_{i,i+1}(\bar{\phi}_{i+1} - \bar{\phi}_i), \quad (2)$$

$$\bar{D}_{i,i+1} = \frac{2 \left(\frac{D_i}{\Delta x_i} \right) \left(\frac{D_{i+1}}{\Delta x_{i+1}} \right)}{\frac{D_i}{\Delta x_i} + \frac{D_{i+1}}{\Delta x_{i+1}}}, \quad (3)$$

A correction factor $\hat{D}_{i,i+1}$ that adjusts the net current to be that of the reference can be introduced as below:

$$\bar{J}_{i,i+1}^{ref} = -\bar{D}_{i,i+1}(\bar{\phi}_{i+1} - \bar{\phi}_i) - \hat{D}_{i,i+1}(\bar{\phi}_{i+1} + \bar{\phi}_i), \quad (4)$$

$$\hat{D}_{i,i+1} = \frac{-\bar{D}_{i,i+1}(\bar{\phi}_{i+1} - \bar{\phi}_i) - \bar{J}_{i,i+1}^{ref}}{(\bar{\phi}_{i+1} + \bar{\phi}_i)}. \quad (5)$$

Since Eq. (1) is a well-defined problem, correction of the net-current provides an equivalency to the reference solution. Hence, a higher-order solution, i.e., reference solution, can be obtained with an acceleration that stems from the simplicity of FDM, hence attaining the name of coarse-mesh finite difference method (CMFD) [3].

2.2 One-Node CMFD Method

The one-node CMFD method introduces two correction factors separately for each node as illustrated in Fig. 2. Through the analogous expression of neutron current as for Eq. (2), one acquires the following equations [4].

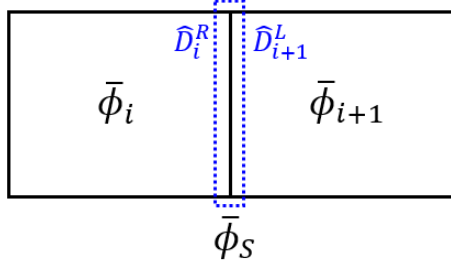


Fig. 2. Visualization of one-node CMFD correction factors.

$$\bar{J}_{i,i+1} = -\frac{2D_i}{\Delta x_i}(\bar{\phi}_s - \bar{\phi}_i) - \frac{2\hat{D}_i^R}{\Delta x_i}(\bar{\phi}_s + \bar{\phi}_i), \quad (6)$$

$$\bar{J}_{i,i+1} = -\frac{2D_{i+1}}{\Delta x_{i+1}}(\bar{\phi}_{i+1} - \bar{\phi}_s) - \frac{2\hat{D}_{i+1}^L}{\Delta x_{i+1}}(\bar{\phi}_s + \bar{\phi}_{i+1}). \quad (7)$$

By equating Eqs. (6) and (7), an expression for the surface flux can be attained.

$$\bar{\phi}_s = \frac{\Delta x_{i+1}(D_i - \hat{D}_i^R)\bar{\phi}_i + \Delta x_i(D_{i+1} + \hat{D}_{i+1}^L)\bar{\phi}_{i+1}}{\Delta x_{i+1}(D_i + \hat{D}_i^R) + \Delta x_i(D_{i+1} - \hat{D}_{i+1}^L)}, \quad (8)$$

where associated correction factors are deduced as below:

$$\hat{D}_i^R = -\frac{\Delta x_i \bar{J}_{i,i+1}^{ref} + 2D_i(\bar{\phi}_s^{ref} - \bar{\phi}_i)}{2(\bar{\phi}_s^{ref} + \bar{\phi}_i)}, \quad (9)$$

$$\hat{D}_{i+1}^L = -\frac{\Delta x_{i+1} \bar{J}_{i,i+1}^{ref} + 2D_{i+1}(\bar{\phi}_{i+1} - \bar{\phi}_s^{ref})}{2(\bar{\phi}_s^{ref} + \bar{\phi}_{i+1})}. \quad (10)$$

It is noteworthy to articulate that Eqs. (9) and (10), which are the correction factors for one-node CMFD, require not only the information of reference current but also the reference surface flux. Comprehensively, procurement of reliable surface flux information is essential concerning the implementation of one-node CMFD acceleration scheme.

2.3 Overall Procedure

A global node-wise reactor eigenvalue problem is considered to attain the multiplication factor and surface-wise incoming partial current. Through the modulation process, such quantities determine both pin-wise fission source and incoming partial current, which result in a formation of local fixed source problem. The pin-wise flux and outgoing partial current are updated accordingly, where the latter quantity could serve as an incoming partial current for consecutive local calculation. Through the homogenization process, the updated local information is impartially transferred to the global calculation. The overall procedure is depicted in Fig. 3.

It is worthwhile to articulate that local calculation is invoked when a prefixed number of global node-wise outer iterations had been performed. Solving local two-node CMFD equation is always entailed by exchange of partial currents, which is referred to as sweeping.

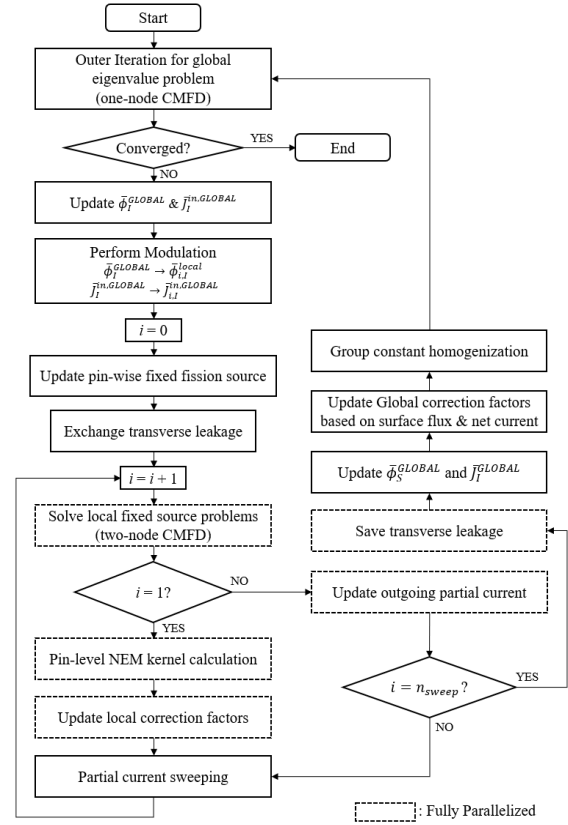


Fig. 3. Overall procedure for HCMFD algorithm

Modulation

$$\bar{\phi}_{i,l}^{local} = \bar{\phi}_i^{GLOBAL} \times \frac{\bar{\phi}_{i,l}^{local}}{\sum_i \bar{\phi}_{i,l}^{local} \cdot \left(\frac{V_{i,l}^{local}}{V_i^{GLOBAL}}\right)}, \quad (11)$$

$$J_{i,l}^{in,local} = J_i^{in,GLOBAL} \times \frac{J_{i,l+1}^{out,local}}{\sum_i J_{i,l+1}^{out,local} \cdot \left(\frac{S_{i,l}^{local}}{S_i^{GLOBAL}}\right)}. \quad (12)$$

Homogenization

$$\bar{\phi}_{S,I}^{GLOBAL} = \sum_i \bar{\phi}_{S,i,l}^{local} \cdot \left(\frac{S_{i,l}^{local}}{S_I^{GLOBAL}}\right), \quad (13)$$

$$J_I^{out,GLOBAL} = \sum_i J_{i,l}^{out,local} \cdot \left(\frac{S_{i,l}^{local}}{S_I^{GLOBAL}}\right), \quad (14)$$

$$\Sigma_{\alpha,I}^{GLOBAL} = \frac{\sum_i \Sigma_{\alpha,i,l}^{local} \cdot \bar{\phi}_{i,l}^{local} \cdot V_{i,l}^{local}}{\sum_i \bar{\phi}_{i,l}^{local} \cdot V_{i,l}^{local}}, \quad (15)$$

α : reaction type, V : volume, S : surface area,
 i : local node index, I : global node index

2.4 Surface Flux Treatment

Implementation of one-node CMFD allows the local problem for each global node to be handled in a parallel manner, which hinges upon global net current and surface flux. The former quantity can be directly

harnessed by the subtraction of outgoing partial currents between interfacing global nodes:

$$\bar{J}_{I,I+1} = \bar{J}_I^{out} - \bar{J}_{I+1}^{out}, \quad (16)$$

where \bar{J}_I^{out} flows from I^{th} node to $(I+1)^{\text{th}}$ node, and \bar{J}_{I+1}^{out} traverses in an opposite direction.

Whereas, there exist several methods to update the global surface flux. As shown in Eq. (13), surface flux for each global node is updated separately, i.e., two different surface flux values exist for every interfacing surface between contiguous global nodes. Calculation of one-node CMFD factors can be directly performed without any further treatment. On the other hand, the interfacing surface flux can be adjusted to their arithmetic average or could be appraised from the diffusion approximation:

$$\bar{\phi}_S = \frac{\bar{\phi}_{S,I} + \bar{\phi}_{S,I+1}}{2}, \quad (17)$$

$$\bar{\phi}_S = 2(\bar{J}_I^{out} + \bar{J}_{I+1}^{out}), \quad (18)$$

where $\bar{\phi}_S$ corresponds to the surface flux between consecutive nodes I and $I+1$.

3. Numerical Results

Figure 4 depicts the MOX-loaded 2D SMR cores that had been considered throughout the presented study, where each fuel assembly consists of 16x16 fuel rods with a pitch of 1.2658 [cm]. The pin-wise 2group homogenized cross-section was acquired from deterministic transport calculation via DeCART2D [5].

A reference solution was obtained by the conventional CMFD accelerated pin-wise nodal expansion method (NEM). For the HCMFD based calculation, the local calculation was invoked for every 5 global iterations. The criterion for convergence was set to be 1E-08 with respect to the L2 norm of the global node-wise fission source error, and every calculation was performed with four 3.1 GHz Intel Core i5 processors.

3.1 Baffle Reflected Core

The convergence behavior for having different numbers of sweeping, i.e., local calculation iteration number, is depicted in Fig 5. The surface flux was either treated based on Eq. (17) or (18), where the former treatment is represented as ‘SF-AVERAGE’ and the latter one as ‘SF-CURRENT’.

Regarding the baffle reflected core, there were no salient distinctions in the convergence behaviour between different approaches, where every method shows a significant reduction in the computing time compared to the pin-wise NEM-CMFD calculation. Table 1 summarizes the elapsed time for performing each calculation.

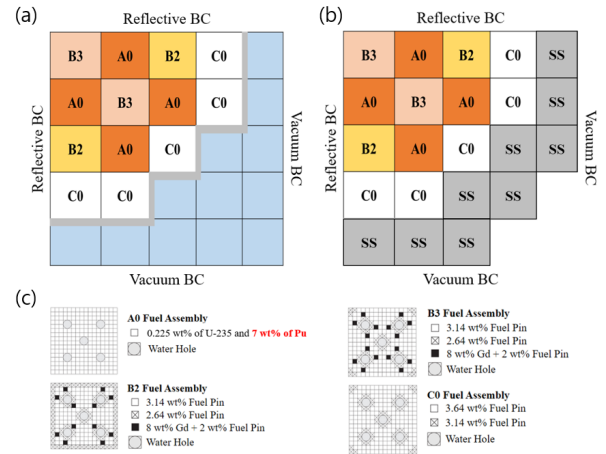


Fig. 4. Illustration of the MOX-loaded cores (a) baffle reflected, (b) stainless-steel reflected, and (c) description of each fuel assembly.

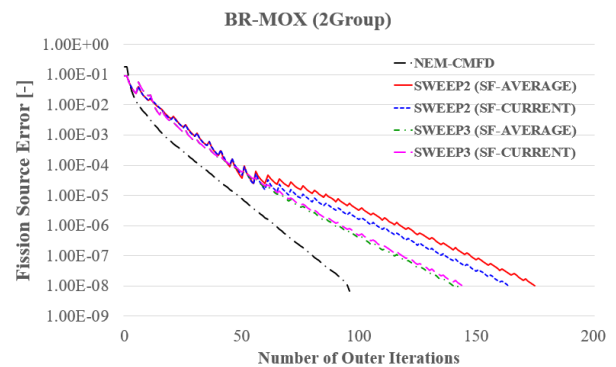


Fig. 5. Convergence behavior for baffle reflected core. Both the number of sweeping procedures performed and surface treatment are exhibited.

Table 1. Computation time and k_{eff} value (Baffle Reflector)

Method	Time (s)	k_{eff}
NEM-CMFD	4.86	1.056064
SWEEP2 / SF-AVERAGE	1.07	1.056064
SWEEP2 / SF-CURRENT	1.01	1.056064
SWEEP3 / SF-AVERAGE	1.05	1.056064
SWEEP3 / SF-CURRENT	1.03	1.056064

3.2 Stainless Steel Reflected Core

Figure 6 illustrates the convergence behaviour for the stainless-steel reflected core. Unlike the baffle reflected core, there exists a noticeable disparity for having sweeping numbers of 2 and 3, where one could observe clear inflection for the former case.

Table 2 enumerates the required computational time for each approach. The reduction in the computing burden for such a core was not much as effective compared to the baffle reflected configuration. Especially, the unstable reduction in the source error hampered the effectiveness of HCMFD acceleration for having a sweeping number of 2. In addition, a non-negligible difference in the computing time was observed for different surface flux treatments with a sweeping number of 3.

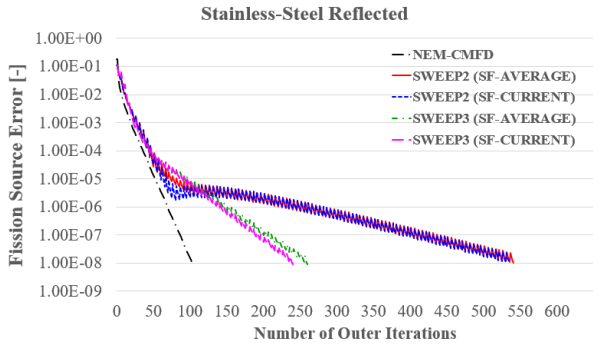


Fig. 6. Convergence behavior for stainless-steel reflected core. Both the number of sweeping procedures performed and surface treatment are exhibited.

Table 2. Computation time and k_{eff} value (SS Reflector)

Method	Time (s)	k_{eff}
NEM-CMFD	4.77	1.075853
SWEEP2 / SF-AVERAGE	2.59	1.075853
SWEEP2 / SF-CURRENT	2.61	1.075853
SWEEP3 / SF-AVERAGE	1.49	1.075853
SWEEP3 / SF-CURRENT	1.39	1.075853

3.3 Adaptive Sweeping

Further increase in the number of sweeping was conducted with a current based assessment of surface flux for the stainless-steel reflected core. Figure 7 exhibits the convergence behavior and the required computing time is shown in Table 3.

From the observation that having a sweeping number of 4 results in the fastest dwindle until the inflection, and sweeping of 3 depicts steady reduction, the following adaptive scheme has been devised.

- step1) Start with n_{sweep} equal to 4.
- step2) Check whether an inflection had occurred or not.
- step3) If inflection point has been encountered, reduce n_{sweep} to 3.

Despite its simplicity, the adaptive scheme successfully provided a further reduction in both computing time and required number of outer iterations as shown in Fig. 8. It could be clearly seen that appropriate local problem consideration significantly affects the overall convergence.

4. Conclusions

The presented paper investigates the variation in the surface treatment strategies accompanied with different sweeping procedures. It has been observed that for the baffle-reflected MOX-loaded core, regardless of the aforementioned considerations, the HCMFD approach noticeably reduces the computing burden.

However, concerning the stainless-steel reflected configuration, an inflection in the convergence have been observed for having a sweeping number of 2. In addition, the diffusion-based surface flux treatment required a smaller number of iterations, although its effectiveness was marginal.

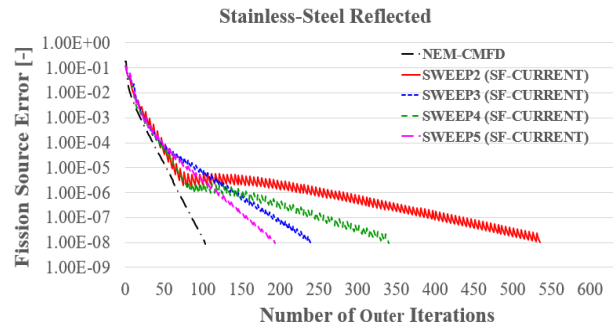


Fig. 7. Convergence behavior for stainless-steel reflected core with a surface flux treatment based on the diffusion theory.

Table 3. Computation time and k_{eff} value (SS Reflector)

Method	Time (s)	k_{eff}
NEM-CMFD	4.77	1.075853
SWEEP2 / SF-CURRENT	2.61	1.075853
SWEEP3 / SF-CURRENT	1.39	1.075853
SWEEP4 / SF-CURRENT	2.20	1.075853
SWEEP5 / SF-CURRENT	1.42	1.075853
ADAPTIVE / SF-CURRENT	1.16	1.075853

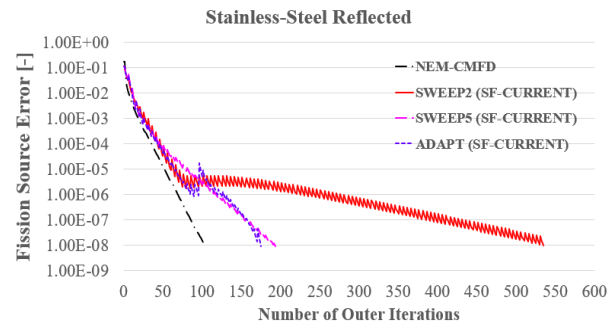


Fig. 8. Convergence behavior for stainless-steel reflected core with adaptive sweeping procedure.

With an adaptive sweeping procedure, the required computational burden dwindled noticeably. Although preliminary, the illustrated result attests to the superior performance of HCMFD over the direct pin-wise CMFD calculation.

AWKNOWLEDGEMENTS

The National Research Foundation of Korea (NRF) Grant funded by the Korean Government (MSIP) (NRF-2016R1A5A1013919) supported this work

REFERENCES

- [1] K. S. Smith (1986), "Assembly Homogenization Techniques of Light Water Reactor Analysis", *Progress in Nuclear Energy*, Vol. 17, No. 3, pp 303-335
- [2] Jaeha Kim, Yonghee Kim (2019), "Development of 3-D HCMFD algorithm for efficient pin-by-pin reactor analysis. *Annals of Nucl Energy* 127, 87-98.
- [3] K. S. Smith (1983), "Nodal method storage reduction by nonlinear iteration", *Trans. Am. Nucl. Soc.* 44, 265.
- [4] H.C. Shin, Y. Kim., 1999. A nonlinear combination of CMFD and FDFM methods, *Proceedings of Korean Nuclear Society Spring Meeting*.
- [5] Y. Cho., *DeCART2D v1.1 User's Manual*, KAERI/UM-40/